Conformational Preferences of Neurotransmitters: Norephedrine and the Adrenaline Analogue, 2-Methylamino-1-phenylethanol

Patrick Butz,[†] Romano T. Kroemer,[‡] Neil A. Macleod,[†] Evan G. Robertson,[†] and John P. Simons*,[†]

Physical and Theoretical Chemistry Laboratory, University of Oxford, South Parks Road, Oxford OX1 3QZ, United Kingdom, and Department of Chemistry, Queen Mary and Westfield College, University of London, Mile End Road, London E1 4NS, United Kingdom

Received: August 30, 2000; In Final Form: November 16, 2000

The conformational preferences of the neurotransmitters (1R2S) norephedrine and 2-methylamino-1-phenylethanol (MAPE) have been examined under free-jet expansion conditions using a combination of laser-induced fluorescence (LIF), mass-selected resonant 2-photon ionization (R2PI), and infrared ion-dip spectroscopy together with ab initio calculations. Comparison of experimental infrared spectra and rotational band contours with ab initio data has allowed a full structural assignment of three conformers in MAPE and two in norephedrine. All five conformers are stabilized by intramolecular hydrogen bonding between the functional groups of the ethanolamine side chain, with the OH group acting as a proton donor. Further stabilizing interactions are provided by NH···π hydrogen bonds and by dispersive interactions between the methyl group of the side chain and the aromatic ring. A delicate balance of these factors controls both the relative stabilities of the conformers and, through cooperative effects, the strength of the primary OH···N hydrogen bond. The existence of a unique IR absorption spectrum for each individual conformer provides a powerful tool for the assignment of molecular conformation.

1. Introduction

The combination of spectroscopic and computational strategies for probing the conformational preferences and supramolecular structures of molecules of biological importance and their molecular clusters, stabilized at low temperatures in the gas phase, is proving to be an extremely powerful one.[1−22] It has been particularly effective in characterizing the structures of a rapidly expanding range of neurotransmitters,[1−15] molecules that act to modify the internal biochemistry of the body. Recent studies have included for example, amino acids,[16−22] monoamines such as phenylethylamine,[1−6,8] amphetamine,[9] and histamine,[14,15] and the ethanolamine, 2-amino-1-phenylethanol (APE).[9] APE is closely related to the family of *ephedra* molecules, an important class of pharmaceuticals.[23,24] Like the ephedra molecules themselves, its flexible side chain allows, in principle, the possibility of a large number of alternative conformations but high-level ab initio calculations indicate a strong preference for those which can support intramolecular hydrogen bonding between the neighboring amino and hydroxyl substituents and, in the event, only two conformers were detected in its jet-cooled, mass-selected, 2-photon ionization (R2PI) spectrum.[9] A combination of rotational band contour analysis, UV 'hole-burning' and IR−UV laser ion-dip spectroscopy, coupled with ab initio computation, led to their structural assignment. As predicted, both were stabilized by OH → NH_2 hydrogen bonding: the *anti*-conformer, with an extended side chain was slightly more stable than its folded, gauche counterpart (in contradiction to the ab initio prediction).

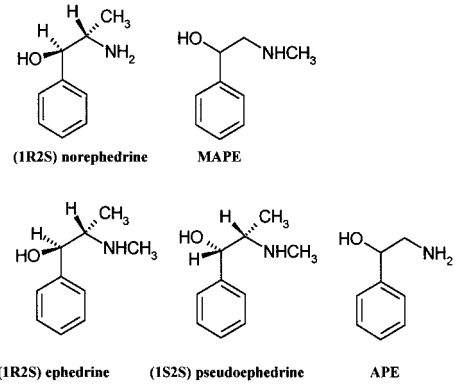

Figure 1. Structures of the molecules of interest.

This work inspired a new study of the conformational landscapes of (1R2S) ephedrine (used as a treatment for asthma) and (1S2S) pseudoephedrine (a powerful decongestant);[13] their structures are shown in Figure 1. Once again all of their most stable (detected) conformers shared the common feature of an intramolecular OH → N hydrogen bond. Their relative stabilities were also controlled, however, by a delicate balance between the intramolecular hydrogen-bonded interaction and dispersive interactions involving the methyl substituents on the side chain, both with each other and with the aromatic ring: because of this the relative conformer stabilities were highly sensitive to the local stereochemistry of the neighboring chiral carbon atoms.

The current paper presents a further extension of this work to include the related molecules, 2-methylamino-1-phenylethanol (MAPE − an analogue of adrenaline), and (1R2S) norephedrine (an appetite suppressor). Their structures are shown in Figure 1. Previous spectroscopic work on both molecules is limited but solution-phase infrared absorption and vibrational circular

* Corresponding author. E-mail: jpsimons@physchem.ox.ac.uk. Fax: 44 1865 275410.
[†] University of Oxford.
[‡] University of London.

10.1021/jp003121u CCC: $20.00
Published on Web 01/19/2001

dichroism (using C_2Cl_4 as the solvent) combined with low-level ab initio calculations on norephedrine,[24] have indicated the presence of several conformers under these conditions, with a range of O−H stretching frequencies indicative of both hydrogen-bonded and free hydroxyl groups.

2. Methods

The systems used for mass-selected resonant 2-photon ionization (R2PI) and laser-induced fluorescence (LIF) experiments are identical to those described previously.[9,13] A free jet expansion of norephedrine or MAPE was generated in a heated pulsed valve (ca. 120 °C) operated with a typical backing pressure of 3 bar of helium. (1R2S) norephedrine and MAPE (racemic mix) were obtained from Fluka (purity >98%) and used without further purification.

IR−UV ion-dip and IR "hole-burn" spectra were obtained using two electronically synchronized YAG-pumped dye lasers. UV radiation was produced by the frequency-doubled output of a Lambda Physik dye laser (FL2002) pumped by the third harmonic of a Nd:YAG laser. Typical UV pulse energies, of the order of 500 μJ, were focused into the ionization region of a time-of-flight mass spectrometer (Jordan) with a 1 m focal length quartz lens. Tunable infrared radiation in the region of 2.8 μm was generated in a $LiNbO_3$ difference frequency module at the output of a YAG-pumped dye laser (Continuum Powerlite and ND6000). Typical IR pulse energies, ca. 2 mJ, were passed through the chamber antiparallel to the UV beam with a 25 cm focal length CaF_2 lens. The IR laser was fired approximately 100 ns *before* the UV laser to deplete the populations of the electronic ground state of the molecule. Two distinct experiments were carried out. The first involved tuning the UV laser onto a specific R2PI feature while the IR laser was scanned over the mid-IR region (ca. 3800−3200 cm^{-1}) to produce an IR−UV ion-dip spectrum of the ground state of the neutral molecule. In the second experiment the opposite configuration was used with the IR laser tuned to an absorption band of a particular conformer and the UV laser scanned to produce an IR hole-burn R2PI spectrum.

LIF spectra were obtained, initially at low resolution (ca. 0.4 cm^{-1}), with the frequency-doubled output of an excimer (Lambda Physik EMG201, XeCl fill) pumped dye laser (Lambda Physik FL3002). Partially resolved rotational band contours were measured using an intracavity Etalon which reduced the bandwidth of the UV laser to ~0.09 cm^{-1}. Band contour simulations were generated using an asymmetric rigid rotor Hamiltonian.[25]

Ab initio calculations were performed using the Gaussian suite of programs.[26] Initial structures of norephedrine and MAPE were based on the seven most stable conformers of APE.[9] Geometries were first optimized at the HF/6-31G* level, and single-point calculations were subsequently performed at the MP2/6-31G* level to determine relative conformer energies. Excited state (S_1) rotational constants and transition dipole moments for the $S_1 \leftarrow S_0$ transition were calculated using the CIS method with a 6-31G* basis set. Vibrational frequencies were calculated using the B3LYP density functional method and a 6-31+G* basis set, which has been found to yield fair agreement with experimental data for similar molecules when scaling factors of 0.9734 for OH stretching modes and 0.956 for NH modes are used.[9,13,17] Further optimizations were carried out at the MP2/6-31+G*, MP2/6-311G** and MP2/6-311+G** levels of theory on the most stable conformers of each molecule.

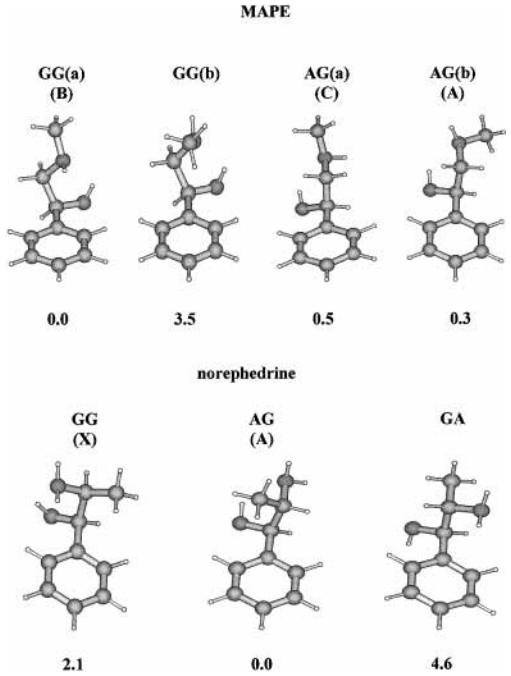

Figure 2. Calculated structures of the lowest lying conformers of MAPE and norephedrine. Quoted energies (kJ mol^{-1}) are from MP2/6-311+G** and include a zero-point correction. Letters in parentheses indicate the assignment of features in the R2PI spectra.

TABLE 1: Ab Initio Structural Parameters and Rotational Constants for the Four Low-Lying Conformers of MAPE

	GG(a)	GG(b)	AG(a)	AG(b)
E_{rel}/kJ mol^{-1} [a]	0.0	6.2	1.7	2.5
E_{rel}/kJ mol^{-1} [b]	3.3	10.2	0.0	0.9
E_{rel}/kJ mol^{-1} [c]	0.0	3.5	0.5	0.3
∠OCCN/deg[c]	−57	−54	54	51
OH···N/pm[c]	217	215	216	212
∠OHN/deg[c]	119	119	119	121
A''/MHz[c]	1855.6	1793.4	2558.4	2723.4
B''/MHz[c]	684.4	797.9	548.8	578.1
C''/MHz[c]	645.3	736.1	515.0	519.5
A'/MHz[d]	1906.3	1800.5	2556.5	2642.6
B'/MHz[d]	655.4	749.3	541.2	571.7
C'/MHz[d]	616.6	698.4	505.6	511.2
μ_a^2:μ_b^2:μ_c^3 [d]	60:36:4	62:25:13	67:32:1	55:45:0
$\lvert\mu_{trans}\rvert \times 10^{30}$/C m[d]	1.20	1.36	0.78	1.00

[a] MP2/6-31G*//HF/6-31G*. [b] B3LYP/6-31+G*. [c] MP2/6-311+G**. [d] CIS/6-31G*.

3. Results

3.1. Ab Initio Calculations. The most stable conformers of norephedrine and MAPE, calculated at the MP2/6-311+G** level of theory, are shown in Figure 2. Structural parameters and rotational constants are also shown in Tables 1 and 2 for MAPE and norephedrine, respectively. The nomenclature is identical to that used previously[9,13] with the conformers identified by the arrangement (anti or gauche) of the CCCN and OCCN atom chains. For MAPE, the presence of an *N*-methyl group doubles the number of conformers due to the facile inversion of the amino group—to distinguish these configurations, an additional designation, (a) or (b), is used.

As with previous studies[9,13] of related molecules the most stable conformers are those which are stabilized by an intramolecular OH → N hydrogen bond between the functional groups of the side chain. For MAPE four such structures are found to lie within 4 kJ mol^{-1} of the global minimum. Structures in which the amino group acts as the proton donor are calculated to be

TABLE 2: Ab Initio Structural Parameters and Rotational Constants for the Three Low-Lying Conformers of Norephedrine

	GG	AG	GA
E_{rel}/kJ mol^{-1} [a]	4.3	0.0	3.0
E_{rel}/kJ mol^{-1} [b]	3.2	0.0	4.6
E_{rel}/kJ mol^{-1} [c]	2.1	0.0	4.6
∠OCCN/deg[c]	55	−54	179
OH···N/pm[c]	213	213	435
∠OHN/deg[c]	119	119	40
A''/MHz[c]	1851.7	2345.1	2200.8
B''/MHz[c]	795.0	683.8	713.6
C''/MHz[c]	717.1	643.7	626.1
A'/MHz[d]	1857.6	2315.3	2212.2
B'/MHz[d]	773.4	667.2	691.4
C'/MHz[d]	691.0	627.3	611.3
μ_a^2:μ_b^2:μ_c^3 [d]	17:81:2	76:22:2	28:71:1
$\lvert\mu_{trans}\rvert \times 10^{30}$/C m[d]	0.59	1.09	0.24

[a] MP2/6-31G*//HF/6-31G*. [b] B3LYP/6-31+G*. [c] MP2/6-311+G**. [d] CIS/6-31G*.

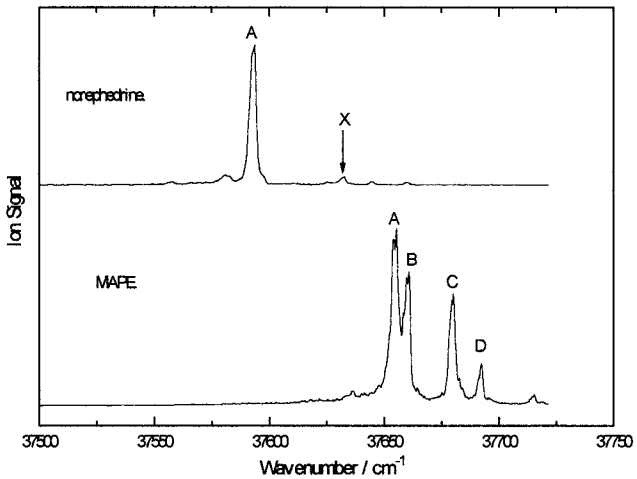

Figure 3. R2PI spectra of MAPE and norephedrine. Both spectra were recorded on the side-chain fragment ion: $(CH(CH_3)NH_2)^+$ for norephedrine and $(CH_2NHCH_3)^+$ for MAPE. Quoted wavenumbers are corrected for vacuum.

substantially less stable. Like APE,[9] the extended AG structures, and the folded GG structures, have very similar energies.

For norephedrine, two of the four analogous conformers (GG and AG) are also found to lie at low energy with AG the global minimum. A third conformer (GA), however, was found to be only slightly less stable than the GG structure. This conformer has an (extended) arrangement of the carbon side chain, similar to the lowest-lying structure of *n*-propylbenzene.[27] The additional stabilization is provided by an NH → π interaction with the aromatic ring similar to that found in the most stable conformers of phenylethylamine[1−6] and amphetamine[8] and in the amino acid, phenylalanine.[17] The orientation of the CH_2−OH group parallels that found in the most stable (and unique) conformer of benzyl alcohol.[11] The relative stability of the GA conformer in norephedrine, where there is no hydrogen bonding between the functional groups *along* the side chain, is in contrast with the conformational landscapes of other similar molecules where the analogous structures lie approximately 10 kJ mol^{-1} above the global minimum.[9,13]

3.2. UV Spectroscopy. Mass-selected resonant two-photon ionization (R2PI) spectra of MAPE and norephedrine in the $S_1 \leftarrow S_0$ origin region are shown in Figure 3. The molecular ions of both species undergo efficient fragmentation and most of the signal is detected in the mass channel, $m/z = 44$, corresponding to $(CH_3CHNH_2)^+$ in norephedrine and $(CH_2NHCH_3)^+$ in MAPE. The extent of fragmentation is ca. 75% for norephedrine and >95% for MAPE, in line with previous work on methyl substituted amines and ethanolamines.[6,8,9,13]

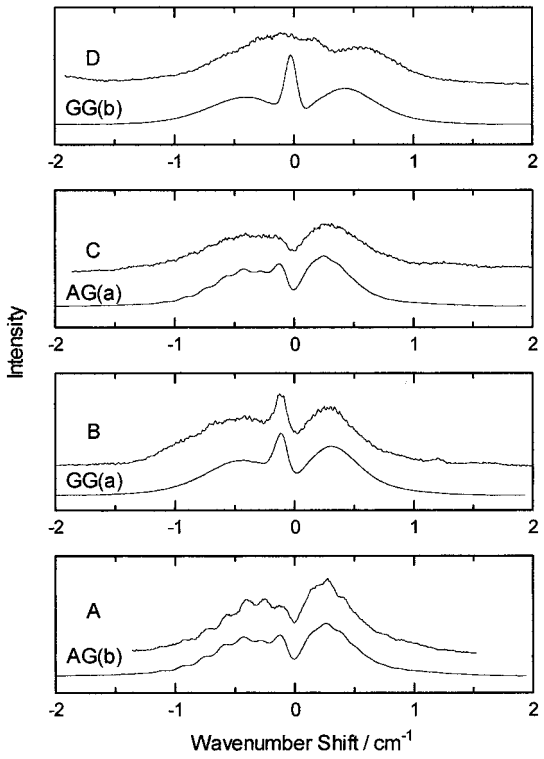

Figure 4. Partially resolved rotational contours of bands A, B, C, and D of MAPE, obtained via fluorescence excitation. Also shown are simulations based on the ab initio data in Table 1, with laser line width = 0.1 cm^{-1}, T_{rot} = 3.5 K for GG(a), GG(b), AG(a), and AG(b).

2-Methylamino-1-phenylethanol. The R2PI spectrum of MAPE shows four prominent features, A (37 655 cm^{-1}), B (37 660 cm^{-1}), C (37 680 cm^{-1}), and D (37 692 cm^{-1}). Their fluorescence excitation rotational band contours are compared in Figure 4 with ab initio simulations for the four low-lying conformers of MAPE, GG(a), GG(b), AG(a), and AG(b). Examination of these contours, and consideration of the calculated relative energies (listed in Table 1), suggest the assignment of B to the origin band of conformer GG(a) and bands A and C to one or other of the structures AG(b) and AG(a); since the two simulations are almost identical, a more definitive assignment, based solely on the band contour analysis, is not possible. Similarly, the band contour of peak D in no way resembles that of the remaining conformer GG(b). Fortunately, each of these difficulties is resolved by the distinctive IR spectral data reported in section 3.3.

Norephedrine. The spectrum of norephedrine is dominated by the single feature, A (37 594 cm^{-1}), but the much weaker peak, X, has also been identified as a second conformer origin through the hole-burning experiments detailed in section 3.3. Their partially resolved rotational band-contours, obtained by fluorescence excitation, are shown in Figure 5 along with contours simulated using ab initio data for each of the three low-lying conformers (GG, AG, and GA) given in Table 2. Comparison of the experimental and simulated contours allows the features A and X to be assigned to the origin bands of the norephedrine conformers AG and GG, respectively, although on this basis alone the alternative assignment of band X to conformer GA cannot be ruled out. These assignments follow the trend of calculated relative energies (see Table 2) and are confirmed by the IR measurements discussed in section 3.3.

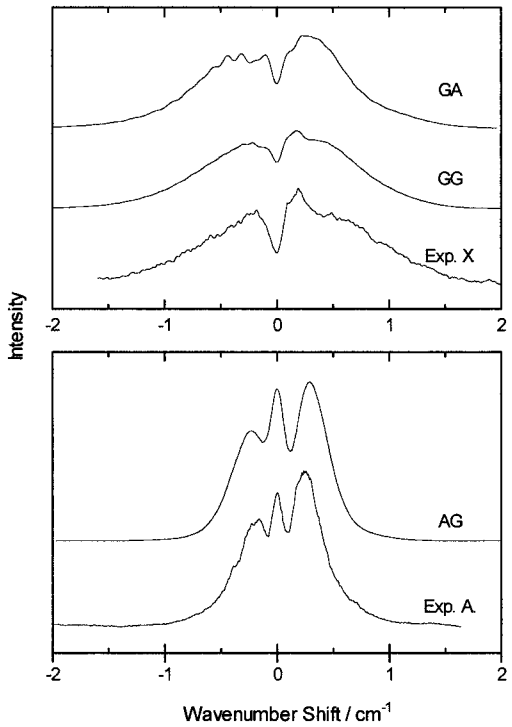

Figure 5. Partially resolved rotational contours of bands A and X of norephedrine, obtained by fluorescence excitation. Also shown are simulations based on the ab initio data in Table 2, with laser line width = 0.1 cm^{-1}, T_{rot} = 1.3 K for AG, 3 K for GG and GA.

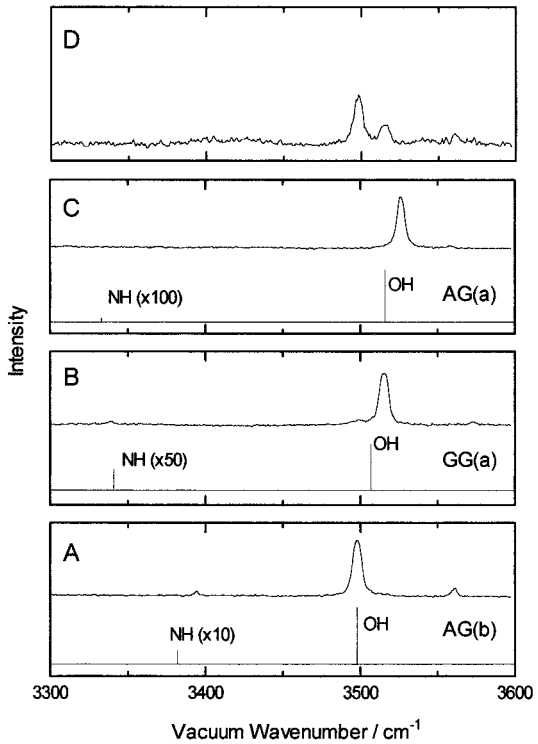

Figure 6. Infrared ion-dip spectra of bands A, B, C, and D of MAPE. Also shown are calculated vibrational spectra based on B3LYP/6-31+G* data (see Table 3) for the three low-lying conformers (GG(a), AG(a), and AG(b)).

3.3. Infrared Ion-Dip Spectroscopy. *2-Methylamino-1-phenylethanol.* IR−UV ion-dip and hole-burn spectra of MAPE are shown in Figures 6 and 7. The R2PI hole-burn spectra recorded with the IR laser successively tuned to the main IR absorption bands associated with the UV features A, B, and C establish their association with three distinct conformers but

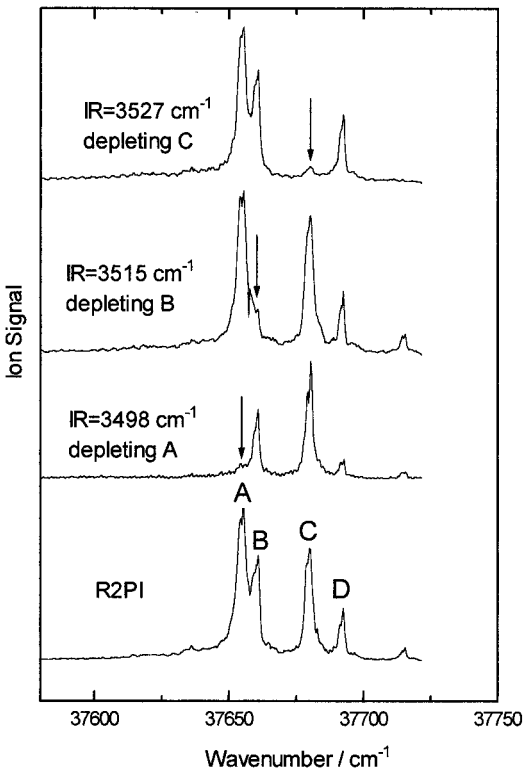

Figure 7. R2PI hole-burn spectra of MAPE in the absence of infrared radiation (lower trace) and when the IR laser is tuned to the absorption bands of features A (3498 cm^{-1}), B (3515 cm^{-1}), and C (3527 cm^{-1}).

when the IR laser is tuned to conformer A, feature D is also depleted. Its association with conformer A is confirmed by the IR−UV ion-dip spectra shown in Figure 6; "conformer D" generates an IR band at the same frequency as conformer A. In addition, a weaker dip is observed at the same frequency as that of conformer B. Hence, peak D in the R2PI spectrum can be assigned to a blended band associated with two overlapping vibronic transitions, based on the conformer origins A and B, which lie too close in energy to be distinguished at the maximum available experimental resolution (ca. 0.1 cm^{-1}). The blending of the two, very different, rotational band contours associated with conformers A and B qualitatively accounts for the unusual band shape seen in Figure 4. In a similar fashion, the IR−UV hole-burn spectrum based upon peak C allows assignment of the weak, blue-shifted feature at 37 715 cm^{-1} to a vibronic transition built upon the conformer band origin C.

The IR ion-dip spectra of conformers A, B, and C all show intense transitions in the region of 3500−3530 cm^{-1} associated with excitation of the O−H stretching mode. Their red shift relative to the O−H stretch frequency in a free alcohol[11,28] (ca. 3650−3680 cm^{-1}) is typical of an intramolecular hydrogen bond in which OH acts as a proton donor to a neighboring amino group. Weaker features observed at lower frequencies, 3394 cm^{-1} (A) and 3340 cm^{-1} (B), are assigned to excitation of the N−H stretching mode. The (scaled) O−H and N−H frequencies, calculated ab initio, for all four low-lying conformers GG(a), GG(b), AG(a), and AG(b) are given in Table 3: stick spectra are also shown for the three lowest lying conformers in Figure 6. The agreement between the relative experimental and calculated vibrational frequencies is excellent, confirming the assignment made in the last section of feature B to structure GG(a) and allowing features A and C to be assigned confidently to the structures AG(b) and AG(a), respectively. The set of additional weak IR bands, shifted by +64, +59, and +32 cm^{-1} relative to the O−H stretch bands of conformers A, B, and C,

TABLE 3: Experimental and Calculated (B3LYP/6-31+G*) Vibrational Frequencies of MAPE[a]

	A	AG(b)	B	GG(a)	C	AG(a)	GG(b)
OH stretch/cm^{-1} [b]	3498	3498 (127)	3515	*3507 (110)*	3527	*3516 (126)*	*3459 (132)*
NH stretch/cm^{-1} [c]	3394	3382 (3)	3340	*3341 (1)*	-	*3333 (0.1)*	*3386 (4)*

[a] The calculated frequencies are in italics. Numbers in parentheses next to the calculated frequencies are the calculated relative intensities of the transition. [b] B3LYP/6-31+G*. Scaling factor of 0.9734 derived from previous work on APE[8] and phenylalanine.[4] [c] B3LYP/6-31+G*. Scaling factor of 0.956 derived from previous work on APE[8] and phenylalanine.[4]

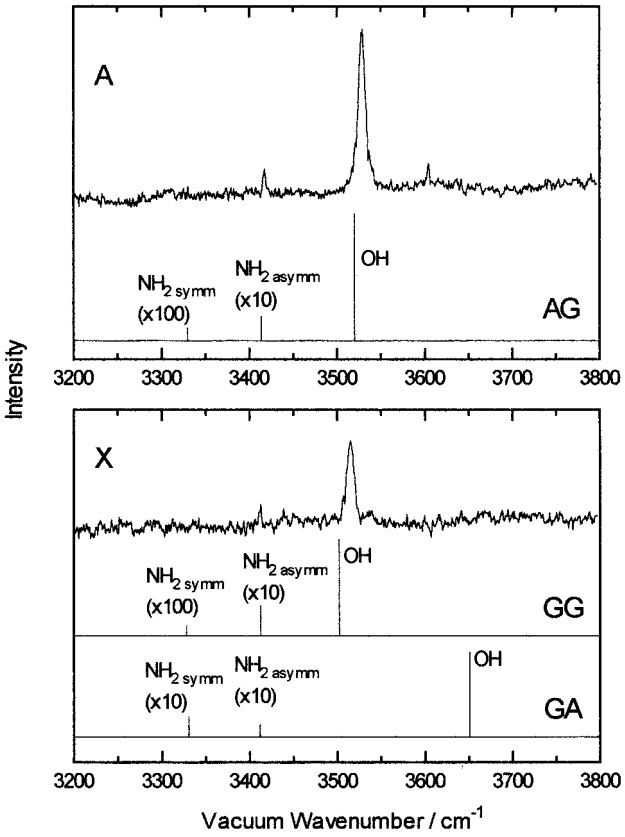

Figure 8. Infrared ion-dip spectra of bands A and X of norephedrine. Also shown are calculated vibrational spectra based on B3LYP/6-31+G* data (see Table 4) for the three low-lying conformers (GG, AG, and GA).

are assigned to combinations of the O−H stretching mode with low-frequency torsional modes of the ethanolamine side chain, on the basis of B3LYP/6-31+G* calculations. These predict frequencies for torsional modes of the side chain which are in excellent agreement with the observed shifts, $\tau(C_\alpha-C_\beta)$in AG-(b) 66 cm^{-1}; $\tau(C_\alpha-C_\beta)$ in GG(a) 58 cm^{-1}; and $\tau(C_1-C_\alpha)$ in AG(a) 32 cm^{-1}. Presumably the OH → N hydrogen bond plays a role in generating the anharmonicity needed for the combination band to be IR allowed. These features have also been observed in ephedrine and pseudoephedrine and in norephedrine (see the next section).

Norephedrine. Figures 8 and 9 show the IR−UV ion-dip and hole-burning R2PI spectra of norephedrine. When the IR laser is tuned to deplete the intensity of peak A, the R2PI hole-burn spectrum reveals band X as a separate conformer origin. The weak R2PI band, shifted −13 cm^{-1} from origin A, is also depleted and is assigned to a hot-band transition associated with a low-frequency vibrational mode. The infrared ion-dip spectra associated with features A and X are both dominated by the intense O−H stretch band (A, 3529 cm^{-1}; and X, 3515 cm^{-1}). The weaker IR bands lying at lower frequency (A, 3417 cm^{-1}; and X, 3414 cm^{-1}) are assigned to the N−H_2 asymmetric stretching mode. As was the case in APE,[9] the symmetric N−H_2 stretch is too weak to be observed.

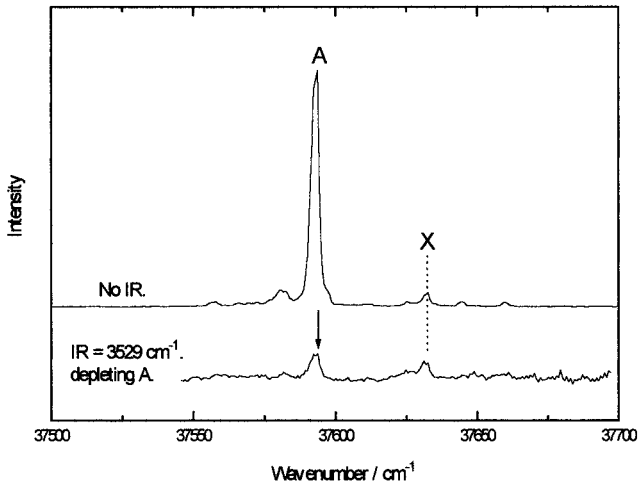

Figure 9. R2PI hole-burn spectra of norephedrine in the absence of IR radiation (upper trace) and with the IR laser is tuned to the absorption band of feature A; 3529 cm^{-1} (lower trace).

TABLE 4: Experimental and Calculated (B3LYP/6-31+G*) Vibrational Frequencies of norephedrine[a]

	A	AG	X	GG	GA
OH stretch/cm^{-1} [b]	3529	*3520 (105)*	3515	*3502 (96)*	*3651 (21)*
NH_2 asymmetric stretch/cm^{-1} [c]	3417	*3414 (2)*	3414	*3413 (3)*	*3412 (0.3)*
NH_2 symmetric stretch/cm^{-1} [c]	-	*3330 (0.1)*	-	*3328 (0.1)*	*3331 (0.5)*

[a] The calculated frequencies are in italics. Numbers in parentheses next to the calculated frequencies are the calculated relative intensities of the transition. [b] B3LYP/6-31+G*. Scaling factor of 0.9734 derived from previous work on APE[8] and phenylalanine.[4] [c] B3LYP/6-31+G*. Scaling factor of 0.956 derived from previous work on APE[8] and phenylalanine.[4]

The scaled O−H and asymmetric N−H_2 vibrational frequencies, calculated ab initio, show excellent agreement with the experimental values (see Figure 8 and Table 4) if features A and X are assigned to the structures AG to GG, respectively. These assignments are also in agreement with those based upon the rotational band contour analysis and the calculated relative energies. The additional weak band in the IR−UV ion dip spectrum of A, shifted +76 cm^{-1} from the O−H stretch vibration is assigned to a combination band involving the O−H stretch and the $\tau(C_\alpha-C_\beta)$ torsional mode (calculated at 76 cm^{-1} for the conformer AG).

4. Discussion

Conformational Preferences. The conformational preferences of the neurotransmitters, MAPE and norephedrine, isolated in the gas phase have been elucidated by a combination of UV rotational band contour analysis, infrared ion-dip spectroscopy, and R2PI hole-burning spectroscopy supported by ab initio calculations. The significant finding is that both of the conformers observed in norephedrine and all three conformers of MAPE are stabilized by an intramolecular hydrogen bond between the functional groups of the ethanolamine side chain, with the OH

group acting as the proton donor. This interaction appears to be a universal feature[9,13] in the most stable ethanolamine structures: similar studies of ephedrine,[13] pseudoephedrine,[13] and 2-amino-1-phenylethanol,[9] conducted in the low-temperature environment of a free jet expansion, have provided no evidence for any contribution from the less stable alternative conformers.

Each of the hydrogen bonds has a similar structure, with OH···N bond lengths lying in the range 205−219 pm and OH....N angles in the range 119°−124° at the MP2/6-311+G** level. These are far from optimum, particularly the OH···N bond angles, which are far from linearity and constrained by the geometry of the side chain. The constraints are reflected in the rather small red shift of the O−H stretching mode (ca.160 cm^{-1} relative to a free alcohol[11,28]). In the phenol−ammonia cluster[29] the favorable, unconstrained geometry leads to an OH···N bond length of 199 pm, a near linear ∠OH···N bond angle and a red shift of 363 cm^{-1}. The red shifts of the O−H stretch bands in APE[9] and MAPE (and also norephedrine) are, perhaps surprisingly, very similar which suggests that methylation of the amino group (or the neighboring methylene group) has little effect on the hydrogen-bonded interaction in their ethanolamine side chains. This is in marked contrast to the situation in clusters of phenol with alkylated amines where a relationship is found between the red shift of the O−H mode and the proton affinity of the amine.[29] The lack of such a dependence for the conformers of APE and MAPE (and norephedrine) can probably be traced to the strained nature of the internal hydrogen bond.

Although the OH···N hydrogen bond exerts a major influence on the conformational landscapes of norephedrine and MAPE, and on those of the ethanolamines in general, it is by no means the only influence. Weaker, but significant, hydrogen-bonded interactions between the (methyl)amino group and the π-system of the ring (analogous to those in 2-phenylethylamine[1−6,8] and, a fortiori, 2-phenylethanol[5,6,10−12]) and dispersive interactions between the methyl groups and the rest of the framework of the molecule can provide additional stabilization and, more importantly, subtly modulate the length and strength of the main hydrogen bond through cooperative effects. Dispersive interactions between the C- and/or *N*-methyl substituents and the π-electron system on the aromatic ring correlate well with the red shifts in the $S_1 \leftarrow S_0$ conformer band origins. In the APE molecule,[9] where there are no methyl substituents, the AG and GG conformer band origins lie at 37 693 and 37 685 cm^{-1} but in the AG(a) conformer of ephedrine,[13] where the C-methyl group lies directly over the ring, the origin band lies at 37 553 cm^{-1}, a red shift of ∼140 cm^{-1}, and in the GG(b) conformer of pseudoephedrine, where the *N*-methyl group lies directly above the ring, the red shift increases to ∼270 cm^{-1}. This "fine-tuning" is also reflected in the sensitivity of the IR absorption spectra to changes in the side-chain conformation, providing a unique "fingerprint" for each conformer and facilitating their individual assignment.

The identification of individual conformers solely on the grounds of a comparison between their calculated relative energies and the relative intensities of their optical spectra rests upon a number of tacit assumptions and may lead to misassignments. MAPE provides an excellent example of this: the relative energies (calculated at the MP2/6-311+G** level) of the three conformers identified experimentally, and also predicted to be the most stable, lie within a range of 0.5 kJ mol^{-1}. Not surprisingly, the origin bands in their R2PI spectra, shown in Figure 4, are all of comparable intensity and it is simply not possible to correlate their relative intensities with their relative populations and relative energies. Many factors may come into play. These can include differences in the relative entropies, and hence free energies of each conformational structure, which may change their relative ordering; a conformational dependence of the lifetime of the excited electronic state, or the magnitude of the transition moment for the $S_1 \leftarrow S_0$ transition; and, perhaps most importantly, the possibility of relaxation of conformers during the supersonic expansion.[15,21,30] Such factors can, and do, have a substantial effect on the intensity distributions in experimental R2PI, LIF and microwave spectra; it has been the *combination* of techniques, including R2PI and LIF spectroscopy, rotational band contour analysis, infrared ion-dip and hole-burn spectroscopy, and ab initio calculation that has enabled the identification and structural assignment of individual conformers to be made at a high level of confidence.

The conformational preferences of APE, MAPE, norephedrine, and the other ephedrine molecules are controlled, in the gas phase, by a complex balance between hydrogen bonding, dispersive, and repulsive interactions. In the physiological realm, where nonbonded interactions between solvent (water) and solute can greatly influence the conformational landscape, the situation would be expected to be even more complex. Gas-phase studies of molecular clusters between water and molecules with flexible side chains (for example APE[9] and *N*-benzylformamide[31]) have shown that the conformational landscape can be greatly influenced by intermolecular hydrogen-bonded interactions. Protonation of the amino group under physiological conditions would have still more dramatic consequences for internal (and external) hydrogen bonding. Even an aprotic solvent can significantly affect the conformational distribution. Norephedrine in C_2Cl_4, for example, displays IR absorption bands and VCD features which indicate both hydrogen-bonded and free hydroxyl groups.[24] Likely candidates for the source of the free O−H vibration are the conformational structures, such as GA and some of the (higher energy) structures in which the amino group acts as proton donor.

5. Conclusions

The conformational preferences of the neurotransmitters norephedrine and 2-methylamino-1-phenylethanol have been studied under free-jet expansion conditions. A combination of R2PI spectroscopy, rotational band contour analysis, and infrared ion-dip spectroscopy coupled with ab initio calculations has allowed the confident assignment of three conformers in MAPE and two in norephedrine. All five experimentally observed conformers owe their high degree of stabilization to an intramolecular OH → N hydrogen bond between the functional groups of the ethanolamine side chain. Further interactions include dispersive effects between the methyl group of the side chain with the aromatic ring and between the (methyl)amino group and the π-system of the ring. Cooperative effects result in unique IR absorption spectra for each conformer. The use of such spectra as fingerprints provides a powerful tool for elucidating the molecular geometry of these flexible, bioactive molecules.

Acknowledgment. We wish to thank the EPSRC (N.A.M., P.B.), Glaxo-Wellcome (P.B.), and the Leverhulme Trust (E.G.R.) for financial support and Professor George Tranter for helpful discussions.

References and Notes

(1) Sipior, J.; The, C. K.; Sulkes, M. *J. Fluoresc.* **1991**, *1*, 41.
(2) Martinez, S. J. III.; Alfano, J. C.; Levy, D. H. *J. Mol. Spectrosc.* **1993**, *158*, 82.
(3) Godfrey, P. D.; Hatherley, L. D.; Brown, R. D. *J. Am. Chem. Soc.* **1995**, *117*, 8204.

(4) Sun, S.; Bernstein, E. R. *J. Am. Chem. Soc.* **1996**, *118*, 5086.
(5) Dickinson, J. A.; Hockridge, M. R.; Kroemer, R. T.; Robertson, E. G.; Simons, J. P.; McCombie, J.; Walker, M. *J. Am. Chem. Soc.* **1998**, *120*, 2622.
(6) Hockridge, M. R.; Robertson, E. G. *J. Phys. Chem. A* **1999**, *103*, 3618.
(7) Unamuno, I.; Fernandez, J. A.; Longarte, A.; Castano, F. *J. Phys. Chem. A* **2000**, *104*, 4364.
(8) Yao, J.; Im, H. S.; Foltin, M.; Bernstein, E. R. *J. Phys. Chem. A* **2000**, *104*, 6117.
(9) Graham, R. J.; Kroemer, R. T.; Mons, M.; Robertson, E. G.; Snoek, L. C.; Simons, J. P. *J. Phys. Chem. A* **1999**, *103*, 9706.
(10) Mons, M.; Robertson, E. G.; Snoek, L. C.; Simons, J. P. *Chem. Phys. Lett.* **1999**, *310*, 423.
(11) Mons, M.; Robertson, E. G.; Simons, J. P. *J. Phys. Chem. A* **2000**, *104*, 1430.
(12) Brown, R. D.; Godfrey, P. D. *J. Phys. Chem. A* **2000**, *104*, 5742.
(13) Butz, P.; Kroemer, R. T.; Macleod, N. A.; Simons, J. P. *J. Phys. Chem.*, in press.
(14) Vogelsanger, B.; Godfrey, P. D.; Brown, R. D. *J. Am. Chem. Soc.* **1991**, *113*, 7864.
(15) Godfrey, P. D.; Brown, R. D. *J. Am. Chem. Soc.* **1998**, *120*, 10724.
(16) Rizzo, T. R.; Park, Y. D.; Peteanu, L. A.; Levy, D. H. *J. Chem. Phys.* **1986**, *84*, 2534.
(17) Piuzzi, F.; Dimicoli, I.; Mons, M.; Tardivel, B.; Zhao, Q. *Chem. Phys. Lett.* **2000**, *320*, 282.
(18) Snoek, L. C.; Robertson, E. G.; Kroemer, R. T.; Simons, J. P. *Chem. Phys. Lett.* **2000**, *321*, 49.
(19) Cohen, R.; Brauer, B.; Nir, E.; Grace, L.; de Vries, M. *J. Phys. Chem. A* **2000**, *104*, 6351.
(20) Godfrey, P. D.; Brown, R. D. *J. Am. Chem. Soc.* **1995**, *117*, 2019.
(21) Godfrey, P. D.; Brown, R. D. *J. Mol. Spectrosc.* **1996**, *376*, 65.
(22) Suenram, R. D.; Lovas, F. J. *J. Am. Chem. Soc.* **1980**, *102*, 7180.
(23) Zigmond, M. J. *Fundamental Neuroscience*; Academic Press: London, 1998.
(24) Freedman, T. B.; Ragunathen, N.; Alexander, S. *Faraday Discuss.* **1994**, *99*, 131.
(25) Hockridge, M. R.; Knight, S. M.; Robertson, E. G.; Simons, J. P.; McCombie, J.; Walker, M. *PCCP* **1999**, *1*, 407.
(26) Frisch, M. J.; Trucks, G. W.; Schlegel, H. B.; Gill, P. M. W.; Johnson, B. G.; Robb, M. A.; Cheeseman, J. R.; Keith, T.; Petersson, G. A.; Montgomery, J. A.; Raghavachari, K.; Al-Laham, M. A.; Zakrzewski, V. G.; Ortiz, J. V.; Foresman, J. B.; Cioslowski, J.; Stefanov, B. B.; Nanayakkara, A.; Challacombe, M.; Peng, C. Y.; Ayala, P. Y.; Chen, W.; Wong, M. W.; Andres, J. L.; Replogle, E. S.; Gomperts, R.; Martin, R. L.; Fox, D. J.; Binkley, J. S.; Defrees, D. J.; Baker, J.; Stewart, J. P.; Head-Gordon, M.; Gonzalez, C.; Pople, J. A. *Gaussian 94*, revision C.3; Gaussian, Inc.: Pittsburgh, PA, 1995.
(27) Dickinson, J. A.; Joireman, P. W.; Kroemer, R. T.; Robertson, E. G.; Simons, J. P. *J. Chem. Soc., Faraday Trans.* **1997**, *93*, 1467.
(28) Provencal, R. A.; Casaes, R. N.; Roth, K.; Paul, J. B.; Chapo, C. N.; Saykally, R. J.; Tschumper, G. S.; Schaefer, H. F., III *J. Phys. Chem. A* **2000**, *104*, 1423.
(29) Iwasaki, A.; Fujii, A.; Watanabe, T.; Ebata, T.; Mikami, N. *J. Phys. Chem.* **1996**, *100*, 16053.
(30) Ruoff, R. S.; Klots, T. D.; Emilsson, T.; Gutowsky, H. S. *J. Chem. Phys.* **1990**, *93*, 3142.
(31) Robertson, E. G.; Hockridge, M. R.; Jelfs, P. D.; Simons, J. P. *J. Phys. Chem. A* **2000**, *104*, 11714.